

Electrostatic interaction effects on the size distribution of self-assembled giant unilamellar vesicles

Mohammad Abu Sayem Karal ^{1,*},[†] Marzuk Ahmed,^{1,*} Victor Levadny,^{2,*} Marina Belaya ³, Md. Kabir Ahamed ¹,
Mostafizur Rahman,¹ and Md. Mostofa Shakil ¹

¹*Department of Physics, Bangladesh University of Engineering and Technology, Dhaka 1000, Bangladesh*

²*Theoretical Problem Center of Physico-Chemical Pharmacology, Russian Academy of Sciences, Moscow 117977, Russia*

³*Department of Mathematics of Russian State University for the Humanities, Moscow GSP-3 125993, Russia*



(Received 23 June 2019; published 9 January 2020)

The influence of electrostatic conditions (salt concentration of the solution and vesicle surface charge density) on the size distribution of self-assembled giant unilamellar vesicles (GUVs) is considered. The membranes of GUVs are synthesized by a mixture of dioleoylphosphatidylglycerol and dioleoylphosphatidylcholine in a physiological buffer using the natural swelling method. The experimental results are presented in the form of a set of histograms. The log-normal distribution is used for statistical treatment of results. It is obtained that the decrease of salt concentration and the increase of vesicle surface charge density of the membranes increase the average size of the GUV population. To explain the experimental results, a theory using the Helmholtz free energy of the system describing the GUV vesiculation is developed. The size distribution histograms and average size of GUVs under various conditions are fitted with the proposed theory. It is shown that the variation of the bending modulus due to changing of electrostatic parameters of the system is the main factor causing a change in the average size of GUVs.

DOI: [10.1103/PhysRevE.101.012404](https://doi.org/10.1103/PhysRevE.101.012404)

I. INTRODUCTION

Lipid molecules dispersed in an aqueous solution form spontaneously a large variety of different bilayer aggregates [1]. If the lipid concentration in the solution is above a threshold level, they self-assemble into aggregates of varying sizes and shapes [2–4]. After some specific manipulations [5] they form closed spherical constructions named unilamellar vesicles (each vesicle has one lipid bilayer) with different vesicle size distributions, depending on the specific conditions of manipulation. The unilamellar vesicles usually are divided into three groups depending on their sizes: small unilamellar vesicles (SUVs) of size 25–50 nm, large unilamellar vesicles (LUVs) of size 50 nm to 10 μm , and giant unilamellar vesicles (GUVs) of size 10 μm or more. The unilamellar vesicles have attracted particular attention of researchers due to their scientific, industrial, and clinical significance. They are considered promising systems for a vast range of industrial and medical applications. In particular, currently they are extensively investigated by medical researchers as tools which can deliver a drug to assured specific body organs [6–8]. On the other hand, the presence of vesicles and vesicle-like structures in a number of biological systems (e.g., those similar to the lipid frame of a cell membrane) has attracted the interest of numerous researchers and scientists studying the biological life processes. This is the reason why, among other things, lipid vesicles are used as model systems to investigate the biophysical principles behind their action as biomembranes

[9]. So, as one can see, a clearer understanding of vesiculation processes is an industrially and scientifically relevant problem. In each specific case of vesicle preparation, a population of vesicles with different sizes arises in a lipid solution. The analysis of the vesicle size distribution in this population provides important information about the vesicle formation process and about lipid bilayer characteristics. There have been a number of experimental and theoretical studies dealing with this problem (see, e.g., [10,11] and references therein) which elucidated the basic principles of the spontaneous lipid vesiculation. In particular, it was shown that the membrane stiffness and bilayer thickness are two important factors that mediate vesicle size distributions. In particular, the essential role of the higher-order terms in the membrane bending energy for vesiculation of nanoscale vesicles has been demonstrated [12]. Currently, it is more or less commonly accepted that the equilibrium size distribution of a vesicle population and the stability of each vesicle in the population are determined by a competition between the total curvature free energy of all vesicles and the various sources of entropy of the system, such as vesicle translation and bilayer undulation.

The size distribution of nanometer vesicles such as SUVs and LUVs was investigated by varying the salts, salt concentrations, and surface charge density [13,14]. It was shown (using self-consistent-field calculations) that the size of vesicles depends on the membrane bending modulus [13]. Among the unilamellar vesicles of various sizes, GUVs have attracted particular interest because, due to their size and shape, they can be visualized using optical microscopes [15–21]. The size of the GUV provides the opportunity to investigate the phenomena occurring at the surface and also inside a single separate vesicle. As a mimic of cells [22], such GUVs were used to investigate quite a few biophysical characteristics

*These authors contributed equally to this work.

[†]Author to whom correspondence should be addressed: asayem221@phy.buet.ac.bd

and phenomena, particularly the elasticity of lipid membranes [23,24], rupture of vesicles [25–28], molecular transport through a pore [29], etc. It is worth noting that for the preparation of GUVs, the natural swelling method (which we use here in our research) is very popular because it makes it possible to obtain oil-free GUVs of different sizes [15–20,25–28]. We emphasize that the main aim of the present study is devoted to the size distribution of GUVs obtained by this method. Additionally, we consider the influence of electrostatic conditions (salt concentration of the solution and vesicle surface charge density in the membranes) of the system on the GUV size distribution, which is relevant for the following reasons. It is well known that electrostatics plays an important role in the functioning of real biological systems. For example, electrostatic effects control the proteins binding to cell membranes, structural changes of membranes, and stability of membranes [30–33]. As we mentioned above, the lipid vesicle is considered as a mimic of the biological membrane of a real cell; hence it is interesting to consider the behavior of such artificial vesicles in conditions corresponding to real biological conditions. In addition, there is the engineering question in industrial and medical industries, namely, how to manage the vesicle size in the process of their production. We suppose that just the electrostatic characteristics of the system can be the proper tool for controlling the distribution to get the specific vesicles size. Therefore, it is necessary to check this assumption.

The structure of the paper is as follows. The biochemical materials and the experimental methods used are described in Sec. II. The electrostatic interaction effects are varied by changing the salt concentration C in buffer solution and the dioleoylphosphatidylglycerol molar fraction X in the membranes of GUVs. The experimental results are presented in Sec. III. To analyze the experimental results statistically, we use the log-normal distribution [34]. In Sec. IV the physical theory is developed to explain the experimental results obtained. The theory based on the Helmholtz free energy of the system is the modification of the approach developed to describe the formation of nanoscale vesicles [12]. In Sec. V A comparison of our theory with the experimental results is presented. Based on these considerations, we conclude that the electrostatic effects are important parameters in determining the sizes of GUVs, and hence they really can be a factor in the manipulation of the formation of GUVs to get the specific size of vesicles.

II. MATERIALS AND METHODS

A. Chemicals and reagents

1,2-dioleoyl-*sn*-glycero-3-phosphotiglycerol (sodium salt) (DOPG) and 1,2-dioleoyl-*sn*-glycero-3-phosphocholine (DOPC) were purchased from Avanti Polar Lipids Inc. (Alabaster, AL). Bovine serum albumin (BSA); piperazine-1,4-bis (2-ethanesulfonic acid) (PIPES); and *O*, *O'*-bis(2-aminoethyl)ethyleneglycol-*N,N,N',N'*-tetraacetic acid (EGTA) were purchased from Sigma-Aldrich (Germany). All the chemicals and reagents were used without further purification.

B. Synthesis and observations of lipid membranes of GUVs

DOPG and DOPC lipids were used to synthesize the GUVs by the natural swelling method [15–17,28]. To investigate the effects of salt concentration C , 40%DOPG/60%DOPC GUVs (where % indicates mol %) were prepared in a buffer (10 mM PIPES, pH 7.0, 1 mM EGTA) containing various concentrations of NaCl with 0.10 M sucrose. The conductivity of this buffer is very similar to that used in our recent experiment on the electrical impedance technique for probing deep organs in the human body [35]. For experiments on surface charge density effects, GUVs of a DOPG and DOPC mixture containing various molar fractions of DOPG, X , were prepared in a buffer containing 150 mM NaCl with 0.10 M sucrose. A mixture of 1 mM DOPG and DOPC (total volume 200 μ l) was placed in a glass vial and dried with a gentle flow of nitrogen gas to produce a thin homogeneous lipid film. The remaining chloroform in the film was removed by placing the vial in a vacuum desiccator overnight. Then 20 μ l Milli-Q water was added to the glass vial and then prehydrated for 8 min at 45 °C. After prehydration, the sample was incubated with 1 ml of buffer containing 0.10 M sucrose for 3.5 h at 37 °C to produce a GUV suspension. At first, 280 μ l of buffer containing 0.10 M glucose (external solution) was transferred into a handmade microchamber. Then 20 μ l aliquot of the GUV suspension (0.10 M sucrose in the buffer as the internal solution) was mixed into the buffer of the microchamber. DOPC GUVs were synthesized in Milli-Q water using the same procedure. To visualize the GUVs in the suspension, a sugar asymmetry between the inside and the outside of the GUVs was created. The GUVs settled down at the bottom of the microchamber due to the density difference of the sugar solution. The difference in refractive indices of the sugar solution enhanced the contrast of GUVs during the observation. To remove the strong attraction between the glass surface and the GUVs, the microchamber and the glass surface were coated with 0.10 wt./vol % BSA dissolved in a buffer containing 0.10 M glucose. After settling down the GUVs in the microchamber, we hold them for 20–25 min to get the equilibrium state of the suspension and then we started the measurements. This time is enough to get the equilibrium distribution as observed before [15–20,25–28,32,36]. The GUVs were observed using an inverted phase contrast microscope (Olympus IX-73, Japan) with a 20 \times objective at 25 ± 1 °C. The GUVs were recorded using a charge-coupled-device camera (Olympus DP22, Japan).

III. RESULTS

A. Effects of salt concentration on the size distribution of GUVs

To investigate the effects of salt concentration C on the size distribution and the average size of GUVs, vesicles were analyzed for the case of $X = 0.4$ using various C . The vesicles with $X = 0.4$ were prepared in a buffer without NaCl (total salt concentration $C = 12$ mM and Debye length $1/\kappa = 2.8$ nm) [25]. Figure 1 shows the experimental results for $C = 12$ mM and $C = 312$ mM. Figure 1(a) shows a typical experimental result of the phase contrast image of GUVs in the suspension for $C = 12$ mM. After measuring the diameters D of 329 GUVs (i.e., number of measured GUVs $N = 329$) from the several phase contrast images in the case of

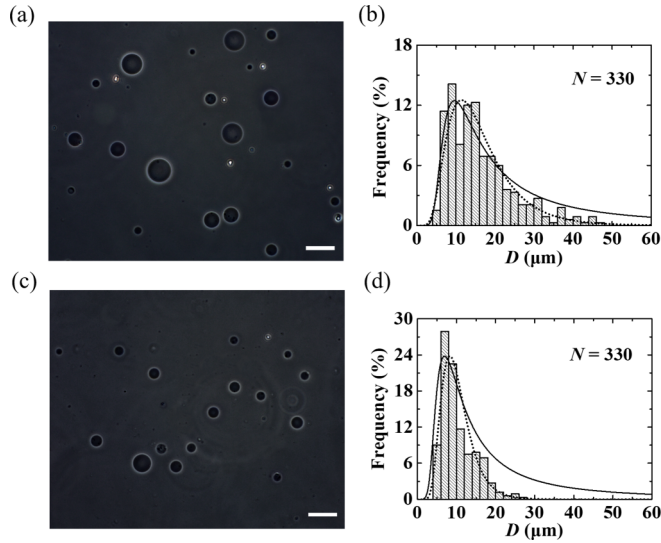


FIG. 1. Effects of salt concentration on the size distribution of GUVs containing $X = 0.4$. (a) Phase contrast image and (b) size distribution histogram at $C = 12$ mM. (c) Phase contrast image and (d) size distribution histogram at $C = 312$ mM. The bar in the images corresponds to $50 \mu\text{m}$. Here N is the number of observed GUVs. The dotted lines show the best-fitting curves corresponding to Eq. (1). The parameters are (b) $\mu = 2.89$ and $\sigma = 0.46$ and (d) $\mu = 2.26$ and $\sigma = 0.38$. The values of R^2 for the fitted curves are (b) 0.94 and (d) 0.95. The solid lines show the theoretical curves corresponding to Eq. (9). The fitting parameters are (b) $K_{\text{ben}} = 36.0 k_B T$, $D_{\text{freq}} = 9.5 \mu\text{m}$, and $L = 1240$ and (d) $K_{\text{ben}} = 16.0 k_B T$, $D_{\text{freq}} = 6.8 \mu\text{m}$, and $L = 1061$. The values of R^2 are (b) 0.66 and (d) 0.75.

$C = 12$ mM, a histogram of the distribution of GUVs was obtained [Fig. 1(b)]. As can be seen from this figure, the histogram is asymmetrical in shape, i.e., a large number of GUVs with diameters greater than $15 \mu\text{m}$ and a small number of GUVs with diameters $4\text{--}14 \mu\text{m}$ are observed. A similar result was also obtained in a second independent experiment (i.e., the total number of experiments was $n = 2$). The result of experiments in the same buffer containing 300 mM NaCl ($C = 312$ mM and $1/\kappa = 0.54$ nm) is shown in Fig. 1(c). The histogram of the GUV's size based on the observation in this case of $N = 330$ is shown in Fig. 1(d), where a small number of GUVs with diameters greater than $15 \mu\text{m}$ and a large number of GUVs with diameters $4\text{--}14 \mu\text{m}$ are shown. A similar result was also obtained in another independent experiment. From a comparison of these histograms one can conclude that, with an increase of C , the size distribution of GUVs shifted to the left, i.e., in the range of small vesicles. In other words, the histogram becomes more asymmetrical. We then analyzed the GUV size distribution for $X = 0.4$ for six other concentrations in the range from $C = 12$ to 400 mM and the proper histograms were obtained. To analyze the experimental results one needs a mathematical description of the histograms obtained. Here we use a well-known log-normal distribution [34]

$$f(D) = \frac{1}{D} \frac{1}{\sigma \sqrt{2\pi}} \exp\left[-\frac{\{\ln(D) - \mu\}^2}{2\sigma^2}\right] \\ = \frac{1}{D} \frac{1}{\sigma \sqrt{2\pi}} \exp\left[-\frac{\{\ln(D/\rho)\}^2}{2\sigma^2}\right], \quad (1)$$

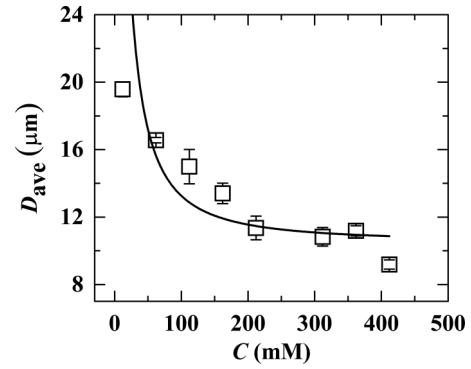


FIG. 2. Average size of GUVs containing $X = 0.4$ at various C obtained from histograms in accordance with Eq. (2). Average values and standard errors of the size for each C were determined from two independent experiments using 300–400 GUVs for each experiment. The solid line shows the theoretical curve corresponding to Eq. (14) with Eq. (15) using $D_{\text{freq}0} = 12.0 \mu\text{m}$, $K_{\text{ben}0} = 17.0 k_B T$, and $\gamma = 2 \text{ mM}^{3/2}$.

where $f(D)$ indicates the frequency of GUVs with diameter D (probability density function), the dimension median ρ (or dimensionless $\mu = \ln \rho$) and σ^2 are the distribution parameters, and μ is the mean of the distribution of $\ln D$. From Eq. (1) the average value of the distribution D_{ave} is [34]

$$D_{\text{ave}} = \int_0^{\infty} D f(D) dD = \exp\left[\mu + \frac{1}{2}\sigma^2\right] \\ = \rho \exp\left(\frac{\sigma^2}{2}\right). \quad (2)$$

The histograms of Figs. 1(b) and 1(d) were fitted with Eq. (1) and the average diameter of the GUVs was obtained using Eq. (2). Using Eq. (2), the average diameter of the GUVs, $D_{\text{ave}1}$, was calculated as $20.0 \mu\text{m}$ at $C = 12$ mM and as $10.3 \mu\text{m}$ at $C = 312$ mM.

Similar experiments were done for the second time and the average diameters of GUVs, $D_{\text{ave}2}$, were calculated; we obtained $19.1 \mu\text{m}$ at $C = 12$ mM and $11.4 \mu\text{m}$ at 312 mM. The average size (average diameter) of the GUVs, $D_{\text{ave}} = (D_{\text{ave}1} + D_{\text{ave}2})/2$, was calculated from two independent experiments (i.e., $n = 2$) using $N = 300\text{--}400$ GUVs in each experiment. The D_{ave} of (19.6 ± 0.4) and $(10.8 \pm 0.6) \mu\text{m}$ (\pm indicating the standard deviation) were obtained for $X = 0.4$ at $C = 12$ and 312 mM, respectively. The dependence of D_{ave} on C obtained in this manner in the whole range of NaCl concentration from $C = 12$ to $C = 412$ mM for $X = 0.4$ is shown in Fig. 2. It can be seen that as the salt concentration in the buffer increases, the average size of the GUVs decreases. The values of D_{ave} at various C are presented in Table I.

As we mentioned above, our results demonstrate the asymmetrical distribution of GUVs by size, which is well described by the log-normal distribution. Note that the approach based on this distribution was previously used for the description of the distribution of a purified GUV suspension [36]. It was also applied to fit the histogram of the persistence length of the endoplasmic reticulum found from a combination of fixed and live cells (human MRC5 lung cells) [37].

TABLE I. Values of the average size of GUVs and the bending modulus of membranes under various conditions.

Effects of salt concentration for $X = 0.40$			Effects of surface charge for $C = 162 \text{ mM}$		
$C \text{ (mM)}$	$D_{\text{ave}} \text{ (}\mu\text{m)}$	$K_{\text{ben}} \text{ (}k_{\text{B}}T)$	X	$D_{\text{ave}} \text{ (}\mu\text{m)}$	$K_{\text{ben}} \text{ (}k_{\text{B}}T)$
12	19.6 ± 0.4	35.9 ± 0.1	0.0 (in Milli-Q)	10.9 ± 0.1	17.0 ± 0.2
62	16.6 ± 0.2	31.3 ± 0.3	0.10	11.9 ± 0.9	18.5 ± 0.5
112	15.0 ± 1.0	27.8 ± 0.4	0.25	15.4 ± 1.4	21.1 ± 0.1
162	13.4 ± 0.6	24.4 ± 0.2	0.40	13.4 ± 0.6	24.4 ± 0.2
212	11.4 ± 0.7	20.5 ± 0.4	0.55	15.0 ± 0.8	26.7 ± 0.3
312	10.8 ± 0.6	16.3 ± 0.3	0.70	16.5 ± 0.3	28.5 ± 0.4
362	11.2 ± 0.3	13.3 ± 0.2	0.90	17.9 ± 0.1	30.1 ± 0.1
412	9.2 ± 0.3	11.1 ± 0.4			

B. Effects of vesicle surface charge on the size distribution of GUVs

The effects of the vesicle surface charge (determined by X) on the GUVs size distribution were investigated. We have analyzed the system under varying X from $X = 0.1$ to 0.9 in the buffer containing $C = 162 \text{ mM}$ (i.e., $1/\kappa = 0.76 \text{ nm}$ [25]). Figure 3 shows the experimental results for two specific values of X , namely, $X = 0.1$ and 0.9 . Figure 3(a) shows a typical experimental result of the phase contrast image of the GUV suspension for $X = 0.1$. The histogram of the distribution of GUVs using $N = 331$ in the case of $X = 0.1$ is shown in Fig. 3(b). It can be seen from the histogram that there is a

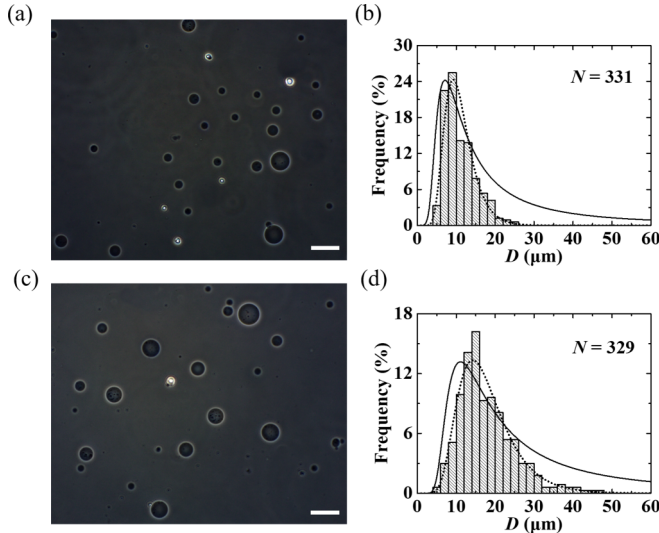


FIG. 3. Effects of DOPG molar fraction on size distribution of DOPG and DOPC GUVs at $C = 162 \text{ mM}$. (a) Phase contrast image and (b) size distribution histogram of the GUV suspension for $X = 0.1$. (c) Phase contrast image and (d) size distribution histogram of the GUV suspension for $X = 0.9$. The bar in the images corresponds to $50 \mu\text{m}$. Here N is the number of observed GUVs. The dotted lines show the best-fitting curves corresponding to Eq. (1). The parameters are (b) $\mu = 2.34$ and $\sigma = 0.34$ and (d) $\mu = 2.81$ and $\sigma = 0.39$. The values of R^2 are (b) 0.90 and (d) 0.97. The solid lines show the theoretical curves corresponding to Eq. (9). The other parameters are (b) $K_{\text{ben}} = 18.0 k_{\text{B}}T$, $D_{\text{freq}} = 7.0 \mu\text{m}$, and $L = 1209$ and (d) $K_{\text{ben}} = 30.0 k_{\text{B}}T$, $D_{\text{freq}} = 11.0 \mu\text{m}$, and $L = 1094$. The values of R^2 are (b) 0.67 and (d) 0.84.

small number of GUVs with diameters greater than $14 \mu\text{m}$ and a large number of GUVs with diameters $4\text{--}14 \mu\text{m}$. A similar result was also obtained in other independent experiments. A typical phase contrast image of the GUVs in the same buffer in the case of $X = 0.9$ is shown in Fig. 3(c) and the corresponding histogram is shown in Fig. 3(d). In the histogram, a large number of GUVs with diameters greater than $12 \mu\text{m}$ and a small number of GUVs with diameters $4\text{--}10 \mu\text{m}$ are observed. A similar result was obtained from other experiments. Therefore, with an increase of X the histogram of the distribution shifted to the right, i.e., in the region of larger GUVs. The histograms of Figs. 3(b) and 3(d) were fitted with Eq. (1) and the average values of the GUVs were obtained [using Eq. (2)] as (11.7 ± 0.9) and $(17.9 \pm 0.1) \mu\text{m}$ for $X = 0.1$ and 0.9 , respectively.

The effects of X on the average size of DOPG and DOPC GUVs in the whole range of X for $C = 162 \text{ mM}$ is shown in Fig. 4. It can be seen that with an increase of X the average size of the GUVs increases. The values of D_{ave} at various X are presented in Table I.

Thus, our results show that the size of a self-assembled GUV is a function of the fraction of charged lipids in the lipid bilayer and the ionic strength of the solution.

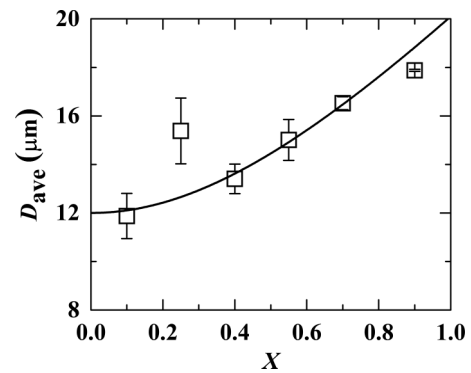


FIG. 4. Average size of DOPG and DOPC GUVs for various X at $C = 162 \text{ mM}$ obtained from histograms in accordance with Eq. (2). Average values and standard errors of the sizes for each X were determined from two independent experiments using 300–350 GUVs for each experiment. The solid line shows the theoretical curve corresponding to Eq. (14) with Eq. (15) using $D_{\text{freq}0} = 10.5 \mu\text{m}$, $K_{\text{ben}0} = 17.0 k_{\text{B}}T$, and $\gamma = 2 \text{ mM}^{3/2}$.

Generalizing these results, one can conclude that with an increase of electrostatic interaction (decrease of C or increase of X) the fraction of large GUVs in the solution increases. As we discuss below, this is a result of the electrostatic effects on the bilayer bending modulus. It is known that at low ionic strength, the curvature energy of a charged lipid bilayer is considerably lower than that of a bilayer carrying lower or no electric charge [13,38,39].

IV. THEORY

A. Free energy of the GUV population

A few theories based on different physical principles have been proposed to explain the process of spontaneous formation of lipid vesicles [12,38,40,41]. It should be noted that these theories mainly considered small vesicles. Here we follow the approach introduced for the formation of nanoscale vesicles [12]. This theory describes the vesiculation of the lipid molecules as interplay between the bending energy of all vesicles and the entropy of the system. Furthermore, the state of the system is determined by the Helmholtz free energy. We modify this approach to describe the formation of micrometer-size GUVs. The molecular dynamics simulation demonstrates that the vesiculation of lipid vesicles starts from small aggregations of lipid molecules, which transform into disklike bilayer structures and then associate with one another and fuse with individual molecules [42,43]. The x-ray-scattering experiments also demonstrated similar phenomena [44]. It was accepted that there is a set of quasistable states of the system with some intermediate structures during the vesicle formation process [45–47]. Hence, before reaching the final equilibrium state (with the final GUV size distribution) the system passes a set of different states with different aggregate size distributions [12]. So our model is based on the following scenario.

We assume that the system (population of lipid molecules) passes a set of states with various size distributions of lipid structures before reaching the final equilibrium state with the final GUV size distribution. Furthermore, we do not consider in detail the full process of GUV formation from lipid molecules; rather we are interested in the last step from some near-final distribution of aggregates (we refer to it as the initial population) to the final GUV distribution. For simplicity, we treat this initial population as a population of N_{init} lipid supramolecular structures. It can be bilayer fragments, SUVs, LUVs, or some curved disklike aggregates [12]. We assume for simplicity that all aggregates in this initial population are exactly the same and we describe it by two parameters: the total number of initial aggregates N_{init} and the surface area of one aggregate S_{init} (which we call the initial vesicle). This assumption means that we describe the real initial population (consisting of lipid structures of different sizes) by the apparent population of some effective structures of equal size. Moreover, the latter corresponds to average size of these structures $D_{\text{init}} = \sqrt{S_{\text{init}}/\pi}$. The initial vesicles transform into different size GUVs due to some process by which the final equilibrium distribution of GUVs by size is achieved. Each GUV in this population is described by a number of initial aggregates m , which compose it. Taking into account that the

total surface of m initial aggregates is mS_{init} , one determines the diameter of m GUVs as $D_m = \sqrt{mS_{\text{init}}/\pi}$. We also assume that each GUV has a spherical (or quasispherical) shape and consists of lipids with zero spontaneous curvature. Generally, the state of such a system under consideration is determined by the Helmholtz free energy G as [12]

$$\begin{aligned} \frac{G(n_m, m)}{k_B T} &= \sum_{m=1}^{N_{\text{init}}} n_m \left[4\pi K_{\text{ben}} \left(1 + \frac{l_c^2}{D_m^2} \right) - \frac{\alpha}{2} \ln \left(\frac{m}{2} \right) \right] \\ &\quad - \left[N_{\text{init}} \ln(\phi N_{\text{init}}) - \sum_{m=1}^{N_{\text{init}}} n_m \ln(m n_m) \right] \\ &\approx \left(4\pi K_{\text{ben}} \sum_{m=1}^{N_{\text{init}}} n_m \right) - \left[N_{\text{init}} \ln(\phi N_{\text{init}}) \right. \\ &\quad \left. - \sum_{m=1}^{N_{\text{init}}} n_m \ln(m n_m) \right], \end{aligned} \quad (3)$$

where m is the number of initial aggregates that compose m GUVs, n_m is the number of m GUVs in the system, K_{ben} is the bending modulus of the membrane in $k_B T$ unit, k_B is the Boltzmann constant, and T is the absolute temperature. The parameter l_c denotes the nonlinear component of K_{ben} , α is the vesicle membrane fluctuation effect on the bending energy, and ϕ is the volume fraction of the initial vesicles in solution. We simplify Eq. (3) by taking into account that $\alpha \sim 6$ and $l_c \sim 10$ nm [12] (while $K_{\text{ben}} \sim 20k_B T$ [23]) and that the characteristic size of GUVs is of the order of $10 \mu\text{m}$ in our experiments. This is the simplified form of the equation we will use below.

The first term in Eq. (3) describes the bending energy of all vesicles (see [48]) in the GUV population and the second term is the contribution of the configurational entropy. Our theory, based on Eq. (3), determines the vesicle size distribution as a result of the interplay between the bending energy of all vesicles and the entropy of the system. It is worth emphasizing that the entropy plays the key role in the determination of the GUV size distribution. A few words about the entropy term of Eq. (3) are in order. The bigger the vesicle size, the smaller the number of vesicles N_{ves} (in the case of fixed $N_{\text{init}} = \text{const}$). Therefore, the number of probable placements of N_{init} (initial aggregates) by the final number of vesicles N_{ves} [i.e., $C_{N_{\text{init}}}^{N_{\text{ves}}} = N_{\text{init}}!/N_{\text{ves}}!(N_{\text{init}} - N_{\text{ves}})!$] in the case of the population of big vesicles (i.e., smaller N_{ves}) is less than in the case of the population of the small ones. This means that the configurational entropy (determined just by $C_{N_{\text{init}}}^{N_{\text{ves}}}$) of the first population is less than that of the second one. Hence, the entropy promotes decreasing of the vesicle size. However, the bending energy of small vesicles is higher than that of big ones. There is a competition between these two free-energy terms: The bending energy aims to increase the vesicle size, but the entropy aims to decrease it. The final size distribution in the equilibrium population is determined by the interplay between these contributions in free energy. It is the reason why the population of lipid vesicles is sometimes called the entropically stabilized population of vesicles [49].

Note the specific role played by the entropy due to the mutual spatial orientation between the initial aggregates in

each vesicle forming this GUV (we call it the orientational entropy for simplicity). It is obvious that these aggregates are more mutually spatially ordered in big vesicles than in smaller ones (in the limit case of the flat bilayer, where all molecules are almost parallel to each other, the spatial ordering is maximal and hence the entropy of such a structure is minimal). The bigger the vesicle size the smaller its orientational entropy contribution in the total free energy of the system. Our previous estimations showed that the main contribution is due to just the configurational entropy. We show below that Eq. (3) describes sufficiently well each specific distribution as well as the histogram transformations upon a change of the electrical parameters (C and X). This is why we do not take into account here the orientational entropy, in order not to overload the theory with secondary cumbersome mathematical expressions.

The following question may arise: How is the electrostatic contribution presented in the expression (3)? The reply is that we put all electrostatic effects in the bending modulus of the membrane. Hence, in our model K_{ben} is a function of salt concentration in solution C and vesicle surface charge density X , i.e., K_{ben} is $K_{\text{ben}}(C, X)$.

We have one more remark dealing with K_{ben} in Eq. (3). Because the vesicle size is not presented in this equation explicitly, one can mistakenly conclude that K_{ben} does not influence the size distribution of vesicles; however, that is not correct. We will show below that the bending modulus K_{ben} affects the total number of vesicles in the system N_{ves} . Thus it affects the vesicle size distribution and hence the average size. We will return to this point in Sec. V.

Equation (3) determines the free energy of the system under consideration for any arbitrary set of $\{n_m, m\}$, i.e., the free energy of the system G is a function of many variables $\{(m_1, m_2, m_3, \dots, N_{\text{init}}), (n_{m1}, n_{m2}, n_{m3}, \dots)\}$. The equilibrium state of the system is determined by the equation

$$\frac{\partial G(n_m, m)}{\partial n_m} = 0 \quad \text{for } (n_m = n_{m1}, n_{m2}, n_{m3}, \dots) \quad (4)$$

under the condition

$$\sum_{m=1}^{N_{\text{init}}} n_m m = N_{\text{init}}. \quad (5)$$

The solution of (4) and (5) is

$$n_m(m) = \frac{N_{\text{init}}\phi}{m} \exp\left[-\frac{4\pi K_{\text{ben}}}{m}\right]. \quad (6)$$

This equation describes the distribution of GUVs in the population by the number m of initial aggregates which compose specific GUV. To use this equation to interpret our experimental results it is necessary to replace in Eq. (6) the nonmeasurable parameter m by the measurable one. In order to do this one first replaces m by $D_m = \sqrt{mS_{\text{init}}/\pi}$ as follows:

$$n_m(D_m) = N_{\text{init}}\phi \frac{S_{\text{init}}}{\pi D_m^2} \exp\left[-\frac{4S_{\text{init}}}{D_m^2} K_{\text{ben}}\right]. \quad (7)$$

Then using the condition $\frac{\partial n_m}{\partial D_m} = 0$, one obtains from Eq. (7) the size of the most frequent GUVs in the system (i.e., the mode of the distribution or, in other words, the most frequent diameter D_{freq})

$$D_{\text{freq}} = 2\sqrt{S_{\text{init}}K_{\text{ben}}}, \quad (8)$$

which can be obtained also from experimental histograms. Using Eq. (8), we replace the nonmeasurable parameter S_{init} by the measurable one D_{freq} in Eq. (7) and obtain the theoretical probability density function $f(D_m)$,

$$f(D_m) = \frac{n_m(D_m)}{\Delta D_m} = \left(\frac{L}{K_{\text{ben}}}\right) \left(\frac{D_{\text{freq}}}{D_m}\right)^2 \exp\left[-\left(\frac{D_{\text{freq}}}{D_m}\right)^2\right], \quad (9)$$

where ΔD_m is the step of the experimental histogram (i.e., $\Delta D_m = 2 \mu\text{m}$ in our case) and $L = N_{\text{init}}\phi/4\pi \Delta D_m$. According to Eq. (9), with the increase of D_m the size distribution shows a sharp increase immediately above the minimum critical size and then follows a long tail as the D_m increases. Such a positively skewed distribution was observed also in other work [50,51] (see the solid line in Fig. 1). Equation (9) has two fitting parameters D_{freq} and K_{ben} (L is normalized parameter). It is necessary to underline that, among other things, one can estimate the values of K_{ben} at different C and X by a comparison of the theoretical Eq. (9) with the experimentally obtained histograms.

B. Average size of GUVs

Generally, the average size of GUVs from Eq. (9) is defined as [52]

$$\begin{aligned} D_{\text{ave}} &= \int_0^{\infty} D_m f(D_m) dD_m \\ &= \left(\frac{L}{K_{\text{ben}}}\right) \int_0^{\infty} \left(\frac{D_{\text{freq}}^2}{D_m}\right) \exp\left[-\left(\frac{D_{\text{freq}}}{D_m}\right)^2\right] dD_m \\ &= -\left(\frac{LD_{\text{freq}}^2}{2K_{\text{ben}}}\right) \text{Ei}\left[-\left(\frac{D_{\text{freq}}}{D_{\text{max}}}\right)^2\right], \end{aligned} \quad (10)$$

where $\text{Ei}(z)$ is the exponential integral function and D_{max} is the size of the greatest vesicle obtained in the experiment. Equation (10) determines the average size of the GUVs in each specific experiment. However, this equation is not convenient for a generalized analysis of the system parameters' influence on the size distribution of vesicles. The integral in Eq. (10) is diverging. Therefore, it is worth presenting Eq. (10) in a form that will make it relatively easy to consider and analyze the influence of the system parameters on the distribution of vesicles by size.

This is why it is worth approximating the integrand in Eq. (10). Taking into account that Eq. (9) gives the positively skewed distributions, we approximate this equation by a log-normal distribution [see Eq. (1)], which also gives the positively skewed distributions whose average value is well defined and known [see Eq. (2)]. By comparing Eqs. (1) and

(9) we obtain

$$\left(\frac{L}{K_{\text{ben}}}\right)\left(\frac{D_{\text{freq}}^2}{D_m^2}\right)\exp\left\{-\frac{D_{\text{freq}}^2}{D_m^2}\right\} \approx \frac{P}{D_m\sigma\sqrt{2\pi}}\exp\left\{-\frac{(\ln D_m - \mu)^2}{2\sigma^2}\right\}. \quad (11)$$

The parameters of the proper log-normal distribution (P , μ , and σ) were obtained from the following conditions: (a) the modes of both distributions have to be the same and (b) the distribution widths at high $1/e$ have to be the same. It was found according to these conditions that $\mu = \ln D_{\text{freq}} + \sigma^2$ and $\sigma = \arcsin h(0.87)/\sqrt{2} = 0.56$ approximate the distribution (10) well and determine its average value D_{ave} as

$$D_{\text{ave}} = \exp\left(\mu + \frac{1}{2}\sigma^2\right) = \exp(\mu)\exp\left(\frac{\sigma^2}{2}\right) = D_{\text{freq}}\exp\left(\frac{3}{2}\sigma^2\right) = D_{\text{freq}}b, \quad (12)$$

where $D_{\text{freq}} = \exp(\mu - \sigma^2)$ and $b = \exp(\frac{3\sigma^2}{2}) = 0.67$. Therefore, D_{ave} in our model is determined [Eq. (12)] by D_{ave} , which is determined by the bending modulus and the size of the initial aggregates [see Eq. (8)].

C. Influence of the membrane bending modulus on the average size of GUVs

Before discussing our results it is necessary to clarify the mechanism of the bending modulus influence on the vesicle size distribution. The first term in Eq. (3) describes the bending energy of vesicles. It can be seen that it does not contain the vesicle size explicitly. At first glance it is not clear how this term describes the bending modulus influence on the vesicle size distribution. To understand this point one needs to take into account that this term contains n_m vesicles composed of m initial aggregates. Therefore, this term describes the bending energy of all vesicles in the population. One should recall that the total number of vesicles in the system $\sum_{m=1}^{N_{\text{init}}} n_m = N_{\text{ves}}$ is not fixed (in contrast to the total number of initial particles $N_{\text{init}} = \text{const}$). The larger the fraction of large vesicles, the smaller the N_{ves} . On the other hand, an increase of K_{ben} results in an increase of the bending energy of each individual vesicle [see the first term in Eq. (3)]; however, the system has the ability to decrease this term by decreasing the total number of vesicles N_{ves} . A smaller number of vesicles means a larger fraction of big vesicles and consequently a bigger average vesicle size D_{ave} , which explains the mechanism of the bending modulus influence on the vesicle size distribution.

As can be seen from Eqs. (8) and (9) (and speculations above) the main physical parameter that influences the vesicle size distribution (and therefore the average size D_{ave}) is the membrane bending modulus K_{ben} . That is why it is worth considering in detail the variations of the average size of GUVs due to the changing of K_{ben} . There have been many studies of the electrostatic effects upon K_{ben} . It was shown that the electrostatic contribution to bending rigidity is independent of geometry [11,53,54]. Moreover, K_{ben} can be determined as

$$K_{\text{ben}} = K_{\text{ben}0} + K_{\text{ben}}^{\text{el}}, \quad (13)$$

where $K_{\text{ben}0}$ is the bending modulus of the bilayer in the case of neutral lipids and $K_{\text{ben}}^{\text{el}}$ is the electrostatic term of the bending modulus of the bilayer, which has been considered from various theoretical perspectives [11,55]. Inserting Eqs. (8) and (13) into Eq. (12), one obtains the expression for D_{ave} ,

$$D_{\text{ave}} = bD_{\text{freq}} = 2b\sqrt{(K_{\text{ben}0} + K_{\text{ben}}^{\text{el}})S_{\text{init}}} = 2b\sqrt{K_{\text{ben}0}S_{\text{init}}}\sqrt{1 + \frac{K_{\text{ben}}^{\text{el}}}{K_{\text{ben}0}}} = bD_{\text{freq}0}\sqrt{1 + \frac{K_{\text{ben}}^{\text{el}}}{K_{\text{ben}0}}}, \quad (14)$$

where $D_{\text{freq}0} = 2\sqrt{K_{\text{ben}0}S_{\text{init}}}$ is the most frequent vesicle size in the case of neutral lipids.

It is worth noting that self-consistent-field calculations have shown a similar result, namely, that there is a strong correlation between the values of membrane rigidity and experimentally determined sizes of vesicles synthesized by the freeze-thaw method [14]. We assumed in Eq. (14) that S_{init} does not depend on K_{ben} . We will show below that this assumption is valid in our system (see Sec. VB).

V. DISCUSSION: COMPARISON OF THE PROPOSED THEORY WITH EXPERIMENTAL RESULTS

A. Fitting of size distribution histograms

In this article we have considered the electrostatic effects on the size distribution of GUVs during spontaneous vesiculation obtained using the natural swelling method. The electrostatic effect was varied by changing the salt concentration in solution and the surface charge density of the membranes. All histograms obtained turned out to be positively skewed distributions, which can be mathematically described well by the classical log-normal distribution. This distribution is widely used to describe phenomena and processes in various sciences, from medicine to geology. The peculiarity of this distribution is that in the systems being analyzed the elements corresponding to the smaller value of the random parameter (which is size of the GUV in our case) prevail. In addition, in such a system the probability of each subsequent event depends on the probability of previous events [12]. For our system, this means that the size of the newly formed GUV depends on the number and size of the GUVs already existing in the system. This is due to the change in entropy of the system. The proposed physical model based on Eq. (9) makes it possible to clarify the physical meaning of the processes occurring in the system during spontaneous vesiculation. In Figs. 1(b), 1(d), 3(b), and 3(d) the solid lines show the theoretical distribution obtained using Eq. (9). It can be seen that the theoretical curves describe the experimental histograms well (only four specific cases are shown in the figures); the coefficient of determination R^2 was 0.66–0.84 in all cases. Therefore, Eq. (9) describes the experimental data well enough and correctly represents the effect of electrostatics on the size distribution of vesicles.

As we already mentioned, Eq. (9) is obtained on the basis of the Helmholtz free energy [see Eq. (3)]. The latter consists of two terms: the energy, determined by the bending energy of all GUVs, and the entropy. If the size of some vesicles increases, the number n_m of corresponding vesicles in the

system decreases and, as a result, the total bending energy of all such vesicles is reduced, as described by the first term in Eq. (3). As for the entropy term, it should be taken into account that the bigger the vesicle size the smaller the number of vesicles N_{ves} . Therefore, the number of probable placements of N_{init} (initial vesicles) by the final number of vesicles N_{ves} (which determines the configuration entropy) in the case of the population of big vesicles is less than in the case of the population of small ones. This means that the configurational entropy of the first population is less than that of the second one. The competition between these two contributions in G [Eq. (3)] determines the equilibrium distribution of the GUVs by sizes.

However, in the region of large vesicles, the theoretical distribution overestimates (compared with experiments) the number of large vesicles. As we noted above, Eq. (9) takes into account only configurational entropy, but not orientational entropy. Because Eq. (9) sufficiently describes each specific distribution (with $R^2 = 0.66\text{--}0.84$) as well as the histogram transformations upon a change of electricity parameters (C and X) and to avoid cumbersome mathematical expressions we do not take into account here the orientation entropy. Since this effect is not taken into account in Eq. (9), the theoretical distribution slightly overestimates the distribution in the region of large vesicle sizes.

We emphasize that for all conditions (different C and X) a positively skewed asymmetric distribution was obtained. This means that in the system under consideration the number of GUVs with size smaller than the average one, D_{ave} , prevails over the number of vesicles with a size larger than D_{ave} . Consequently, the system prefers a small GUVs and therefore, as follows from Eq. (3) and the above speculations, the entropy term prevails over the energy one. That is why such spontaneous vesiculation is called entropically stabilized. It is worth mentioning one more thing that contributes to the shift of the distribution in the region of small quantities. As far back as 1941, Kolmogorov considered a similar problem in geology (distribution of particle sizes during crushing) and showed that in such systems the probability of collisions between particles also has a certain value. The probability of collision of small particles with other particles is substantially less than that for large particles [56]. Since the redistribution of particle sizes in the system occurs as a result of particle collisions between themselves, the lifetime of a particular particle of small size is longer than that of a large particle. This effect also contributes to the appearance in the equilibrium distribution of a larger fraction of small particles compared to that of large particles.

The solid lines in Figs. 1(b) and 1(d) correspond to the theoretical Eq. (9) for $X = 0.4$ at $C = 12$ and 312 mM, respectively. From the fitted curves, values of K_{ben} of $36.0k_{\text{B}}T$ [Fig. 1(b)] and $16.0k_{\text{B}}T$ [Fig. 1(d)] were obtained. Average values of K_{ben} of $(35.9 \pm 0.1)k_{\text{B}}T$ and $(16.3 \pm 0.3)k_{\text{B}}T$ for $C = 12$ and 312 mM, respectively, were obtained. Values of R^2 of 0.66 [Fig. 1(b)] and 0.75 [Fig. 1(d)] were obtained.

The size distribution histograms for $C = 162$ mM at various X are shown in Figs. 3(b) and 3(d), which were also fitted by Eq. (9). From the fitted curves (solid lines), the values of K_{ben} of $18.0k_{\text{B}}T$ and $30.0k_{\text{B}}T$ for $X = 0.1$ and 0.9 at $C = 162$ mM, respectively, were obtained. Average values of K_{ben} of $(18.5 \pm 0.5)k_{\text{B}}T$ for $X = 0.1$ and $(30.1 \pm 0.1)k_{\text{B}}T$

for $X = 0.9$ at $C = 162$ mM were obtained. Values of R^2 of 0.67 [Fig. 3(b)] and 0.84 [Fig. 3(d)] were obtained. Hence the average value of K_{ben} varied with C and X . Using the same procedure, a value of K_{ben} of $(17.0 \pm 0.2)k_{\text{B}}T$ for pure DOPC GUVs was obtained, which is similar to that obtained using the micropipette aspiration technique, $(20 \pm 0.5)k_{\text{B}}T$ [23]. Therefore, as the electrostatic interaction increases (increase of X or decrease of C) the values of K_{ben} increase. The values of K_{ben} at various C and X are provided in Table I.

B. Average size of GUVs vs the bending modulus of the lipid bilayer

As we indicated above, the main fitting parameter of the theoretical model is K_{ben} . It allows us to estimate the value of K_{ben} in our experiments, based on experimental histograms and theoretical model. Here we clarify how the bending modulus influences the vesicle size distribution. The first term in Eq. (3) describe the bending energy of all vesicles. It can be seen that it does not contain the vesicle size explicitly. At first glance it is not clear how this term describes the bending modulus influence on the vesicle size distribution. This term contains also the number of vesicles n_m in each population of m vesicles. Therefore, this term describes the bending energy of all vesicles. It should be recalled that the total number of vesicles in the system $N_{\text{ves}} = \sum_{m=1}^{N_{\text{init}}} n_m$ is not fixed (in contrast to the total number of initial particles $N_{\text{init}} = \text{const}$).

Hence N_{ves} in the equilibrium state of the system under consideration corresponds [as it follows from Eqs. (4) and (5)] to the minimum free energy $G(n_m, m)$. The small the number of vesicles in the final equilibrium state of the system the smaller the total bending energy of the system. An increase in K_{ben} results in an increase in the bending energy of each individual vesicle [see first term in Eq. (3)]; however, the system is able to decrease this term during the transformation process by decreasing N_{ves} . As a result of collisions between vesicles, some of them fuse, and therefore N_{ves} decreases, the fraction of big vesicles increases, and the average size of the vesicles in the system increases. This explains how the bending modulus influences the GUV distribution and the average size of the vesicles.

We obtained K_{ben} in our experiments in the range of $16k_{\text{B}}T\text{--}36k_{\text{B}}T$ (Figs. 1 and 3) from the fitting of experimental results by the theoretical Eq. (9). The values of K_{ben} obtained from such fittings are of the same order as the values of K_{ben} for the PC membrane [23] and for PG-PC membrane [57,58]. We assumed above that the average size of vesicles in the initial population S_{init} does not depend on K_{ben} . This means that in our model D_{ave} is proportional only to $\sqrt{K_{\text{ben}}}$, i.e., $D_{\text{ave}} = (2b\sqrt{S_{\text{init}}})\sqrt{K_{\text{ben}}} = \text{const}\sqrt{K_{\text{ben}}}$ [see Eq. (14)]. The following question arises: Does this assumption correspond to real systems? To consider this question we plotted the dependences of $D_{\text{ave}}(C, X)$ and $\sqrt{K_{\text{ben}}}(C, X)$ in the same graph as shown in Fig. 5. It can be seen that D_{ave} is really proportional to $\sqrt{K_{\text{ben}}}$, as it follows from Eq. (14). The appropriate constants are equal to $(2.9 \pm 0.1) \mu\text{m}/(k_{\text{B}}T)^{1/2}$ in Fig. 5(a) for various C at $X = 0.4$ and $(3.0 \pm 0.1) \mu\text{m}/(k_{\text{B}}T)^{1/2}$ in Fig. 5(b) for various X at $C = 162$ mM. Hence one can conclude that the above-mentioned assumption is valid. Figure 5 and Eq. (14) show that if K_{ben} decreases, D_{ave} in the system also decreases.

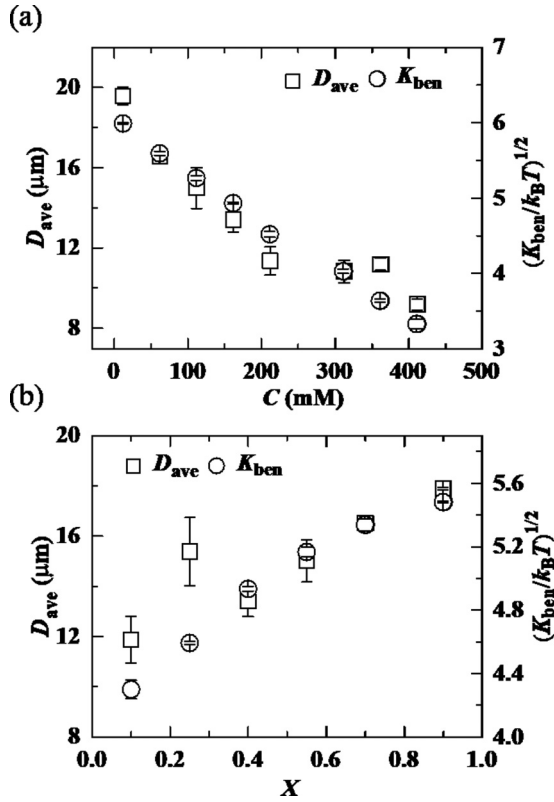


FIG. 5. Relationship between the average size D_{ave} [obtained from histograms in accordance with Eq. (2)] and the bending modulus of the GUV bilayer K_{ben} [obtained from histograms in accordance with Eq. (9)]. (a) Effects of C on D_{ave} and K_{ben} for $X = 0.4$. (b) Effects of X on D_{ave} and K_{ben} at $C = 162$ mM. Average values and standard errors were determined from two independent experiments.

This phenomenon can be easily explained in the framework of Eq. (3). If K_{ben} decreases the bending energy of small vesicles also decreases; therefore, the fraction of such vesicles in the population increases and hence the average size of all vesicles decreases.

C. Fittings of the dependence of the GUV average size on electrostatic interaction

Our results demonstrate that, as the electrostatic interaction increases the values of K_{ben} increase. The size distribution histograms for $C = 162$ mM at various X are shown in Figs. 3(b) and 3(d). From the fitted curves (solid lines), values of K_{ben} of $(18.5 \pm 0.5)k_B T$ and $(30.1 \pm 0.1)k_B T$ for $X = 0.1$ and 0.9 , respectively, were obtained. It is known that electrostatic conditions in the lipid bilayer system influence the bilayer bending rigidity [11]. In particular, a significant enhancement of the bending rigidity of membranes due to charge effects has been established [39]. Measurements based on the fluctuation spectroscopy of giant vesicles showed a decrease of K_{ben} in the presence of various types of salts [59]. The effect of NaCl on K_{ben} of palmitoylphosphocholine membranes exhibited a decrease of K_{ben} from $39k_B T$ to $32k_B T$ due to NaCl concentration changes from 0 to 100 mM [59]. In contrast, incorporation in the bilayer of phosphatidylcholine vesicles of a small fraction (10 mol %) of negatively charged

phosphatidylglycerol results in an approximately three-fold increase of K_{ben} compared to that of the pure phosphatidylcholine membrane [60]. Therefore, these measurements support our result that as the electrostatic interaction increases, K_{ben} also increases.

Taking into account that we have shown that the size distribution and average size of GUVs are determined by K_{ben} [Eqs. (9) and (14)] and that our experimental results demonstrate a significant dependence of the GUV size on the surface charge density and ionic strength of a solution (Figs. 2 and 4), we can say that our results also demonstrate the dependence of the bilayer bending rigidity on electrostatics. It is worth considering this point in detail. For this one has to determine the expression describing the dependence of K_{ben} , i.e., $K_{ben}(C, X)$.

There have been many studies on the effect of electrostatics upon K_{ben} . Moreover, the problem has been analyzed in the framework of various theoretical approaches [14,38,53,61–65]. A substantial number of theoretical studies have addressed the effect of the surface charge density and ionic strength of a solution on the membrane bending rigidity [53,66,67]. It has been shown that the rise in the bending rigidity with increasing fraction of charged species can be connected to the stronger repulsion in the bilayer plane (in particular, between the polar heads of charged lipids), which effectively suppresses the membrane undulations and thus increases the membrane rigidity. The presence of an electric double layer surrounding a charged membrane also affects the bilayer bending rigidity [38]. However, in spite of many studies, at present there is no commonly accepted interpretation of this problem. It was shown that K_{ben} more or less generally increases with an increase of X and decrease of C . Moreover, such dependences of K_{ben}^{el} can be described as a function of C and X as [53,54,61,67]

$$K_{ben}^{el} = \text{const} \frac{\Omega^2}{\kappa^3} = \gamma \frac{X^2}{\sqrt{C^3}}, \quad (15)$$

where the Debye length $\kappa^{-1} = \frac{0.304}{\sqrt{C}}$ nm and Ω is the surface charge density of vesicles. We use this expression for interpretation and fitting of our results in which γ is used as a fitting parameter. The solid lines in Figs. 2 and 4 demonstrate the theoretical curves corresponding to Eqs. (14) and (15) for two specific cases, namely, the dependence $D_{ave}(C)$ for $X = 0.4$ (Fig. 2) and the dependence $D_{ave}(X)$ for $C = 162$ mM (Fig. 4). The experimental points in these figures were obtained from histograms in accordance with Eq. (2) by the method described above. The satisfactory fitting of theoretical curves to experimental data can be seen. We emphasize that despite the fact that Figs. 2 and 4 correspond to totally different experimental conditions (variation of C in one case and variation of X in the other), the fitting of the experimental data by theoretical Eq. (14) with (15) was obtained with the same fitting parameters ($K_{ben0} = 17.0k_B T$ and $\gamma = 2 \text{ mM}^{3/2}$) in both cases. The fitting parameters in Fig. 2 were $D_{freq0} = 12.0 \mu\text{m}$, $K_{ben0} = 17.0k_B T$, and $b = 0.67$ and in Fig. 4 they were $D_{freq0} = 10.5 \mu\text{m}$, $K_{ben0} = 17.0k_B T$, and $b = 0.67$. This means once more that the theory developed herein satisfactorily describes the real processes in the system under consideration.

VI. CONCLUSION

In this paper we considered the effects of electrostatic interactions on the spontaneous formation of GUVs obtained using the natural swelling method. The results were presented as histograms describing the GUV size distribution. The GUV size distributions in the case of different ionic concentrations in solution and different surface charge densities of membranes were examined. All histograms were described very well by a classical log-normal distribution with positively skewed asymmetry. The positively skewed distribution manifests that the number of GUVs with sizes smaller than the average one prevails over the number of vesicles with a size larger than the average size. Based on our theory, we concluded that the positively skewed asymmetry means that the entropy contribution in the free energy prevails over the vesicle bending energy contribution. We have found that with an increase of electrostatic interactions (i.e., decrease of salt concentration or increase of surface charge density) the peak of the histogram shifts to right, i.e., in the region of large vesicles. This means that with an increase of electrostatic interactions the fraction of large GUVs in the solution increases. Hence our results demonstrate that an increase of electrostatic interactions in the system results in an increase of bending energy of vesicles. To explain our experimental results we developed a theory that will help clarify the essence of the physical processes occurring in the system under considera-

tion. We modified the model of Huang *et al.* [12] made for the nanoscale vesicle for our micrometer-scale system. The key assumption of our theory is that we postulate the existence of a certain initial population of lipid bilayer aggregates. Using the experimental results, we have evaluated some parameters of these initial aggregates in accordance with our theory. We obtained also that the general form of GUV size distribution is controlled by the entropy contribution in the total free energy, but the specific distribution is determined by the bending modulus of the membrane.

ACKNOWLEDGMENTS

This work was supported partly by Ministry of Science and Technology (Grants No. 39.00.0000.09.02.69.16-17/Phy's-370, No. 39.00.0000.09.06.79.2017/Phy's-450, and No. 39.00.0000.09.14.009.2019/Phy's-7), Ministry of Education (Grants No. 7.20.0000.004.033.020.2016.1478 and No. 37.20.0000.004.033.020.2016.1053), ICT Division (Grant No. 39.00.0000.028.33.105.18-5), Directorate of Advisory, Extension and Research Services, BUET (Grant No. R-01/2017/2310-73), and University Grants Commission (Grant No. UGC/ST/Phys-9/2017) of Bangladesh to M.A.S.K. M.A. would like to acknowledge the Ministry of Science and Technology, Bangladesh for providing support through a fellowship (Grant No. 39.00.0000.012.002.03.18-23).

The authors declare no conflict of interest.

-
- [1] R. G. Laughlin, *The Aqueous Phase Behavior of Surfactants* (Academic, London, 1994).
- [2] K. Kita-Tokarczyk, J. Grumelard, T. Haeefe, and W. Meier, *Polymer* **46**, 3540 (2005).
- [3] S. Segota and D. Tezak, *Adv. Colloid Interface Sci.* **121**, 51 (2006).
- [4] K. Holmberg, B. Jönsson, B. Kronberg, and B. Lindman, *Surfactants and Polymers in Aqueous Solution* (Wiley, Chichester, 2002).
- [5] N. Karami, E. Moghimipour, and A. Salimi, *Asian J. Pharm.* **12**, S31 (2018).
- [6] T. M. Allen and P. R. Cullis, *Adv. Drug Deliv. Rev.* **65**, 36 (2013).
- [7] Y. Malam, M. Loizidou, and A. M. Seifalian, *Trends Pharmacol. Sci.* **30**, 592 (2009).
- [8] T. Lian and R. J. Ho, *J. Pharm. Sci.* **90**, 667 (2001).
- [9] U. Iqbal, H. Albaghdadi, M.-P. Nieh, U. I. Tuor, Z. Mester, D. Stanimirovic, J. Katsaras, and A. Abulrob, *Nanotechnology* **22**, 195102 (2011).
- [10] V. Guida, *Adv. Colloid Interface Sci.* **161**, 77 (2010).
- [11] E. Sackmann, in *Structure and Dynamics of Membranes: From Cells to Vesicles*, edited by R. Lipowsky and E. Sackmann, Handbook of Biological Physics Vol. 1 (Elsevier, North Holland, 1995), pp. 213–304.
- [12] C. Huang, D. Quinn, Y. Sadovsky, S. Suresh, and K. J. Hsia, *Proc. Natl. Acad. Sci. USA* **114**, 2910 (2017).
- [13] M. M. A. E. Claessens, B. F. van Oort, F. A. M. Leermakers, F. A. Hoekstra, and M. A. Cohen Stuart, *Biophys. J.* **87**, 3882 (2004).
- [14] M. M. A. E. Claessens, B. F. van Oort, F. A. M. Leermakers, F. A. Hoekstra, and M. A. Cohen Stuart, *Phys. Rev. E* **76**, 011903 (2007).
- [15] M. A. S. Karal, J. M. Alam, T. Takahashi, V. Levadny, and M. Yamazaki, *Langmuir* **31**, 3391 (2015).
- [16] M. Hasan, M. A. S. Karal, V. Levadny, and M. Yamazaki, *Langmuir* **34**, 3349 (2018).
- [17] S. Sharmin, M. Z. Islam, M. A. S. Karal, S. U. A. Shibly, H. Dohra, and M. Yamazaki, *Biochemistry* **55**, 4154 (2016).
- [18] M. Z. Islam, J. M. Alam, Y. Tamba, M. A. S. Karal, and M. Yamazaki, *Phys. Chem. Chem. Phys.* **16**, 15752 (2014).
- [19] S. U. Alam Shibly, C. Ghatak, M. A. S. Karal, M. Moniruzzaman, and M. Yamazaki, *Biophys. J.* **111**, 2190 (2016).
- [20] Y. Tamba, H. Ariyama, V. Levadny, and M. Yamazaki, *J. Phys. Chem. B* **114**, 12018 (2010).
- [21] M. C. Blosser, B. G. Horst, and S. L. Keller, *Soft Matter* **12**, 7364 (2016).
- [22] M. M. Zaman, M. A. S. Karal, M. N. I. Khan, A. R. M. Tareq, S. Ahammed, M. Akter, A. Hossain, and A. K. M. A. Ullah, *ChemistrySelect* **4**, 7824 (2019).
- [23] W. Rawicz, K. C. Olbrich, T. McIntosh, D. Needham, and E. Evans, *Biophys. J.* **79**, 328 (2000).
- [24] E. Evans, V. Heinrich, F. Ludwig, and W. Rawicz, *Biophys. J.* **85**, 2342 (2003).
- [25] M. A. S. Karal, V. Levadny, T.-a. Tsuboi, M. Belaya, and M. Yamazaki, *Phys. Rev. E* **92**, 012708 (2015).
- [26] M. A. S. Karal, V. Levadny, and M. Yamazaki, *Phys. Chem. Chem. Phys.* **18**, 13487 (2016).

- [27] M. A. S. Karal and M. Yamazaki, *J. Chem. Phys.* **143**, 081103 (2015).
- [28] M. A. S. Karal, M. K. Ahamed, M. Rahman, M. Ahmed, M. M. Shakil, and K. S. Rabbani, *Eur. Biophys. J.* **48**, 731 (2019).
- [29] M. A. S. Karal, M. K. Islam, and Z. B. Mahbub, *Eur. Biophys. J.* (2019), doi: [10.1007/s00249-019-01412-0](https://doi.org/10.1007/s00249-019-01412-0).
- [30] M. Zaslhoff, *Nature (London)* **415**, 389 (2002).
- [31] S. McLaughlin and D. Murray, *Nature (London)* **438**, 605 (2005).
- [32] Y. Tamba and M. Yamazaki, *J. Phys. Chem. B* **113**, 4846 (2009).
- [33] S. D. Shoemaker and T. K. Vanderlick, *Biophys. J.* **83**, 2007 (2002).
- [34] N. L. Johnson, S. Kotz, and N. Balakrishnan, *Continuous Univariate Distributions*, 2nd ed. (Wiley, New York, 1994).
- [35] S. K. Roy, M. A. S. Karal, M. A. Kadir, and K. S. Rabbani, *Eur. Biophys. J.* **48**, 711 (2019).
- [36] M. A. S. Karal, M. Rahman, M. K. Ahamed, S. U. A. Shibly, M. Ahmed, and M. M. Shakil, *Eur. Biophys. J.* **48**, 349 (2019).
- [37] P. Georgiades, V. J. Allan, G. D. Wright, P. G. Woodman, P. Udommai, M. A. Chung, and T. A. Waigh, *Sci. Rep.* **7**, 16474 (2017).
- [38] M. Winterhalter and W. Helfrich, *J. Phys. Chem.* **96**, 327 (1992).
- [39] V. Vitkova, J. Genova, O. Finogenova, Y. Ermakov, M. D. Mitov, and I. Bivas, *C. R. Acad. Bulg. Sci. Sci. Math. Nat.* **57**, 25 (2004).
- [40] S. A. Safran, P. A. Pincus, D. Andelman, and F. C. MacKintosh, *Phys. Rev. A* **43**, 1071 (1991).
- [41] J. Leng, S. U. Egelhaaf, and M. E. Cates, *Biophys. J.* **85**, 1624 (2003).
- [42] H. Noguchi and G. Gompper, *J. Chem. Phys.* **125**, 164908 (2006).
- [43] H. Yuan, C. Huang, J. Li, G. Lykotrafitis, and S. Zhang, *Phys. Rev. E* **82**, 011905 (2010).
- [44] T. M. Weiss, T. Narayanan, C. Wolf, M. Gradzielski, P. Panine, S. Finet, and W. I. Hsueh, *Phys. Rev. Lett.* **94**, 038303 (2005).
- [45] D. M. Small, S. A. Penkett, and D. Chapman, *BBA—Lipid. Lipid. Met.* **176**, 178 (1969).
- [46] N. A. Mazer, G. B. Benedek, and M. C. Carey, *Biochemistry* **19**, 601 (1980).
- [47] D. D. Lasic, *Biochem. J.* **256**, 1 (1988).
- [48] W. Helfrich, *J. Phys. (Paris)* **47**, 321 (1986).
- [49] M. M. A. E. Claessens, F. A. M. Leermakers, F. A. Hoekstra, and M. A. Cohen Stuart, *Langmuir* **23**, 6315 (2007).
- [50] R. V. Venetić, J. Leunissen-Bijvelt, A. J. Verkleij, and P. H. J. T. Ververgaert, *J. Microsc.* **118**, 401 (1980).
- [51] G. Maulucci, M. De Spirito, G. Arcovito, F. Boffi, A. C. Castellano, and G. Briganti, *Biophys. J.* **88**, 3545 (2005).
- [52] L. D. Landau and E. M. Lifshitz, *Statistical Physics*, 3rd ed., Course of Theoretical Physics Vol. 5 (Butterworth-Heinemann, Oxford, 1980).
- [53] M. Winterhalter and W. Helfrich, *J. Phys. Chem.* **92**, 6865 (1988).
- [54] D. Bensimon, F. David, S. Leibler, and A. Pumir, *J. Phys. (Paris)* **51**, 689 (1990).
- [55] R. Bradbury and M. Nagao, *Soft Matter* **12**, 9383 (2016).
- [56] A. N. Shiriyayev, *Selected Works of A. N. Kolmogorov: Volume II: Probability Theory and Mathematical Statistics* (Springer, Netherlands, Houten, 2012).
- [57] D. Marsh, *Biophys. J.* **70**, 2248 (1996).
- [58] D. Marsh, *Biophys. J.* **73**, 865 (1997).
- [59] R. Dimova, *Adv. Colloid Interface Sci.* **208**, 225 (2014).
- [60] O. Mertins and R. Dimova, *Langmuir* **29**, 14552 (2013).
- [61] H. N. W. Lekkerkerker, *Phys. Stat. Mech. Appl.* **159**, 319 (1989).
- [62] J. L. Harden, C. Marques, J. F. Joanny, and D. Andelman, *Langmuir* **8**, 1170 (1992).
- [63] A. Fogden, J. Daicic, D. J. Mitchell, and B. W. Ninham, *Phys. Stat. Mech. Appl.* **234**, 167 (1996).
- [64] L. M. Bergström, *Langmuir* **22**, 3678 (2006).
- [65] R. Messina, *J. Phys.: Condens. Matter* **21**, 199801 (2008).
- [66] P. Pincus, J.-F. Joanny, and D. Andelman, *Europhys. Lett.* **11**, 763 (1990).
- [67] S. May, *J. Chem. Phys.* **105**, 8314 (1996).